Mortezapour *et al.*
Protection and Control of Modern Power Systems (2022) 7:42
https://doi.org/10.1186/s41601-022-00263-w

Protection and Control of Modern Power Systems

ORIGINAL RESEARCH Open Access

A new hybrid control technique for operation of DC microgrid under islanded operating mode

Vahid Mortezapour[1], Sajjad Golshannavaz[2*], Edris Pouresmaeil[3] and Amin Yazdaninejadi[4]

Abstract

This study proposes a novel combined primary and secondary control approach for direct current microgrids, specifically in islanded mode. In primary control, this approach establishes an appropriate load power sharing between the distributed energy resources based on their rated power. Simultaneously, it considers the load voltage deviation and provides satisfactory voltage regulation in the secondary control loop. The proposed primary control is based on an efficient droop mechanism that only deploys the local variable measurements, so as to overcome the side effects caused by communication delays. In the case of secondary control, two different methods are devised. In the first, low bandwidth communication links are used to establish the minimum required data transfer between the converters. The effect of communication delay is further explored. The second method excludes any communication link and only uses local variables. Accordingly, a self-sufficient control loop is devised without any communication requirement. The proposed control notions are investigated in MATLAB/Simulink platform to highlight system performance. The results demonstrate that both proposed approaches can effectively compensate for the voltage deviation due to the primary control task. Detailed comparisons of the two methods are also provided.

Keywords: Hybrid control technique, Modern power system, DC microgrid, Islanded operating mode

1 Introduction

The technical and economic merits of distributed energy resources (DERs) such as solar photovoltaic, wind turbines, battery storage systems, etc. in power systems, have given rise to significant interest in microgrid (MG) developments at regional levels. The MG benefits include enhancements in power system reliability, resilience, economics, security, and sustainability along with significant reductions in transmission system congestion and deferral of power system expansion [1]. However, these benefits are challenged by several technical issues [2]. MGs can be categorized into two main classes, namely the alternative current (AC) and direct current (DC) types. DC-MGs have several notable advantages over the AC [3, 4], e.g., no skin effect nor power quality issues in DC-MGs, no concern regarding frequency control, and simpler power flow equations. Thanks to these features, DC-MGs contribute to higher efficiency, increased reliability, safety, and redundancy. As well as these technical merits, it also involves less implementation and operational costs [5–9]. In DC-MGs, the generated power of DERs is DC or is converted to DC through power electronics converters. DC-MGs should be controlled such that they can operate in both islanded and grid-connected operating modes [10].

In DC-MGs, two different methods are available to establish the proposed control approach. The first deploys communication links to transfer the required data between the embedded elements and the control unit. For instance, centralized control approaches require such connections [11, 12]. To implement a novel power

*Correspondence: s.golshannavaz@urmia.ac.ir
[2] Electrical Engineering Department, Urmia University, 11Km SERO Road, Urmia City, Iran
Full list of author information is available at the end of the article

routing algorithm for a cluster of DC-MGs in a meshed network, communication links have been deployed in [13, 14]. In general, application of communication links is not an economic approach and degrades reliability. In the second method, there is no communication link and each DER is controlled based on its local variables. In this way, data transfer between the DERs is avoided and they are operated in a decentralized manner. One of the most renowned decentralized approaches is the droop control approach which deploys the converter output voltage and current signals for control purposes [15]. As renewable energy resources are featured with very low or zero inherent inertia, this issue should be satisfied virtually through effective droop control [16]. There are different droop mechanisms proposed in the literature. One of the main issues of the proposed droop-based approaches is the voltage drop due to connection and virtual droop resistances [17]. To eliminate the voltage drop occurring in primary droop control, a secondary control loop is contemplated to return the bus voltage to the nominal value. Different methods have been proposed for addressing this issue in the literature.

In MGs, secondary control is also performed with two different approaches, namely centralized and decentralized [18]. In the centralized approach, the voltage compensation command is sent from the MG central controller (MGCC) to the primary controller through low-bandwidth communication (LBC) links [19, 20]. This approach is in line with a technical drawback in which the MGCC is not highly reliable and resilient and may bear an inherent single-point-of-failure. By contrast, the distributed secondary control is implemented in the local controllers and the information used in the local secondary control scheme is exchanged via LBC networks [21]. This can avoid the impact of single-point-of-failure in the centralized secondary control. However, the effect of line resistances has not been comprehensively considered. Moreover, the current sharing accuracy enhancement is only realized by using larger droop coefficients. There is a lot of research dedicated to primary and secondary control loops to yield effective and appropriate control of DC-MGs within which not only an effective power sharing task is guaranteed but also the DC bus voltage is kept at acceptable levels [22, 23]. The point to be considered is that the secondary control applied to MG is dependent on its primary controller. Accordingly, if the primary controller varies, a proper secondary controller should be designed.

This paper proposes a hybrid control approach based on primary and secondary controls for islanded DC-MGs. It first provides an appropriate load power sharing task between the DERs, and subsequently compensates for the load voltage deviations. The proposed primary control approach is based on a generalized mathematical representation of DER equivalent circuits, one which takes into account the presence of cable resistances. The developed primary control approach is based on that proposed in [24] which innovatively considers the sources with different ratings and also the transmission lines with different connection impedances. This approach has been shown to outperform the others for the task of power sharing between the available resources. Following the primary control task, two different methods are developed for secondary control of DERs. The first is established based on LBC links whereas the second deploys only the local variables and eliminates the communication delays. Therefore, in the case of failure in communication links, the second one can play a backup role with a short delay. Each approach is thoroughly explored throughout the study and the corresponding results are discussed in detail.

The rest of this paper is organized as follows: Sect. 2 addresses the proposed primary control approach along with its mathematical basis. Two different methods are then developed in Sect. 3 to realize an appropriate secondary control on DER converters, while the modelling issues and technical requirements of these methods are also considered in this section. Simulation studies are conducted in Sect. 4 to evaluate the performance of the proposed control approaches. Concluding remarks are then provided in Sect. 5.

2 Applied primary control

Figure 1 illustrates a general circuit representation of a DC-MG. As shown, a set of loads and resources form an islanded MG where an effective control system maintains the voltage at an acceptable level and also shares the power between the resources considering

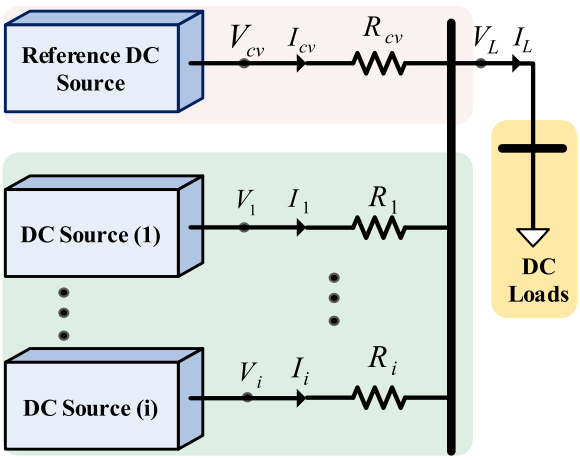

Fig. 1 General representation of a DC-MG

their power ratings. The implemented primary control approach is an effective recently developed one. The substantial fundamentals of this approach have been comprehensively described by the same research team in a recent paper [22]. A brief overview of this study outlines that the output voltage of one of the converters is assumed to be constant and the output voltages of the remaining converters are determined with reference to the constant voltage. The main control mission is to share the load power between the converters considering their rated capacities and in an appropriate manner. Let us assume that the active power rating of the i^{th} DER converter has the following relation to the active power rating of the DER with constant voltage, as:

$$P_i = K_i P_{CV} \tag{1}$$

Here, the converter which is treated with a constant voltage is symbolized with subscripts "*cv*". Note that (1) can be rewritten in the form of (2) based on the voltage and current signals. (3) is formed with respect to the circuit developed in Fig. 1.

$$V_i I_i = K_i V_{CV} I_{CV} \tag{2}$$

$$P_i = K_i P_{CV} \tag{3}$$

where I_i and V_i are the output current and voltage of the *ith* converter, respectively. I_{cv} and V_{cv} are the output current and voltage of the converter with constant voltage, respectively.

As clarified, (1–3) are devised to establish an appropriate power sharing task between the converters. Substituting (2) in (3) yields the following V-I droop characteristics for the *ith* converter:

$$V_i = V_{cv} \frac{V_{cv} + R_i I_i}{V_{cv} + \frac{R_{cv}}{K_i} I_i} \tag{4}$$

Here, R_i is the impedance of the cable connecting the *ith* converter to the load bus, and R_{cv} is the impedance of the cable connecting the converter with constant voltage to the load bus. In this way, the block diagram depicted in Fig. 2 is launched for the proposed primary control approach. As can be seen, if V_{cv} is known, the remaining converters deploy the local current measurements at their terminals to calculate the desired reference

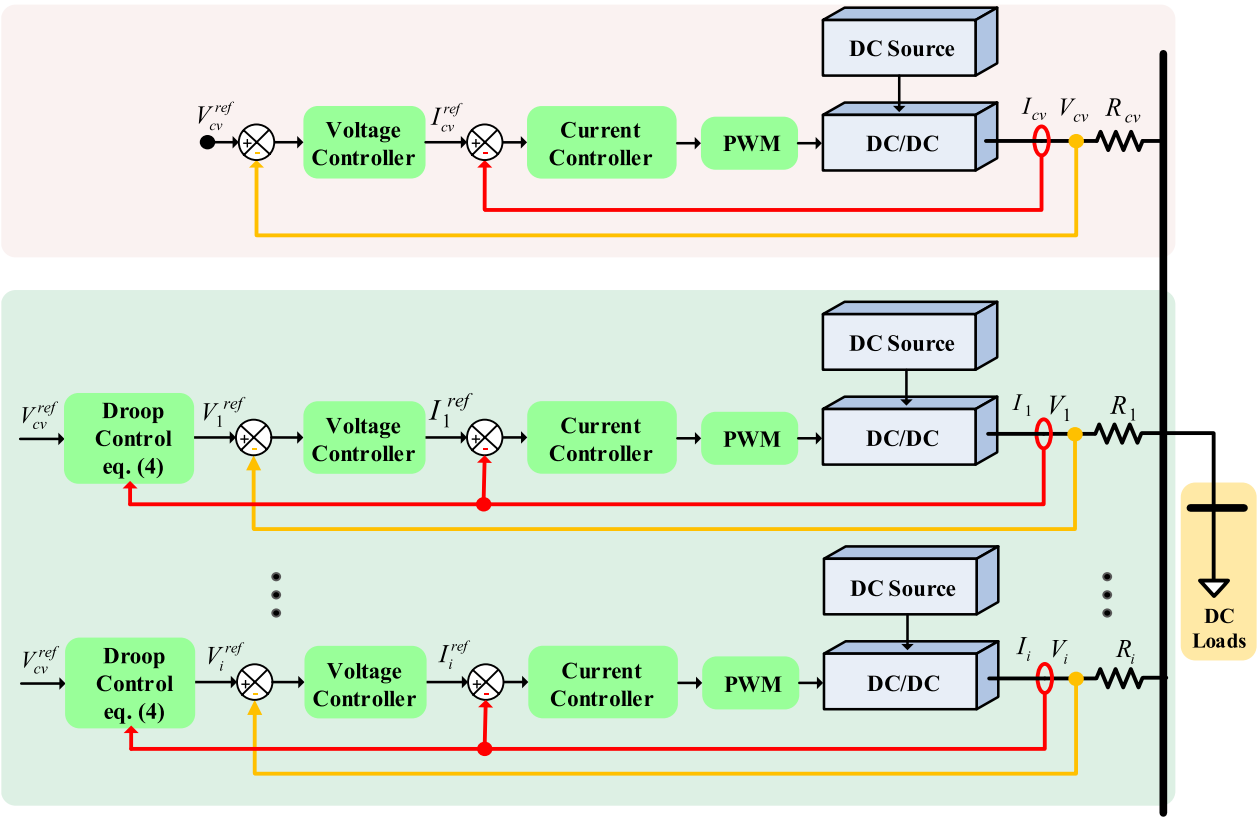

Fig. 2 Block diagram of the proposed primary control approach

voltages. Then, the measured voltage and current signals are passed through the corresponding voltage and current controllers to generate the required control signals for that specific converter.

3 The proposed secondary control approaches

The secondary controller targets mitigation of voltage deviations against the rated values. Following the primary control procedure, the load voltage might not be tuned exactly at the rated value. To overcome the existing fluctuations and regulate the load voltage, the reference bus voltage denoted by subscripts "cv" should be treated as varying with its output current. The following statement is hence considered:

$$V_{cv}^{new} = V_n + R_{cv} I_{cv}^{new} \tag{5}$$

where V_n refers to the nominal load bus voltage. If (5) is included in the control process, the load voltage is kept at its rated value continuously such that the power sharing is also conducted properly. However, the remaining converters need to be informed of the updated constant voltage at the reference bus, namely V_{CV}^{new}. To this end, two different secondary control approaches are proposed including application of an LBC link and without any communication link. Both approaches are discussed in detail in the following subsections.

3.1 Application of LBC link

Deployment of LBC links is due to lower cost and increased reliability in MGs. In this study, such an application is deemed to maintain the load bus bar voltage at the rated value. In this approach, the updated constant voltage of the reference bus that is determined in (5) is broadcasted to the DERs through LBC links. Figure 3 demonstrates the interconnection of DERs and the communication links. To model the communication time delay in this approach, a suitable transfer function, which has been commonly used in related literature, such as [22, 25, 26], is considered:

$$G_d = \frac{1}{1 + \tau s} \tag{6}$$

where τ represents the time delay of the LBC link in seconds. Although it has been clarified in the preceding explanations, it is worth mentioning that this communication link is only deployed to transfer the updated value of the voltage of the converter with constant voltage to the adjacent DERs, while the other required signals are measured locally. Likewise, the corresponding control actions are performed in a local manner. Accordingly, this approach provides an acceptable level of reliability. In the presence of communication delays and errors,

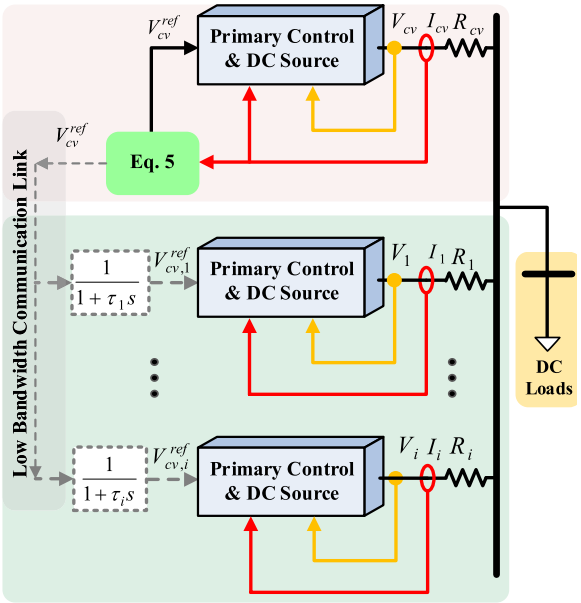

Fig. 3 The proposed secondary control approach based on LBC link

although the proposed approach demonstrates acceptable performance, it might encounter a reduced precision. In the proposed approach, the DERs are only in connection with the source with constant-voltage and receive this reference value. Such an approach reduces the transferred data to the minimum in comparison with the previous methods. Accordingly, not only the system complexity and its implementation cost decrease, but also the reliability of the communication infrastructure highly increases.

3.2 Secondary control without communication links

In this approach, the primary control is implemented within which the reference bus voltage is kept constant and the output voltage of the remaining converters is determined with respect to the reference bus. Without using the LBC links, the voltage deviation occurring in the primary control loop is then compensated for. To this end, the relevant constant voltage should be changed such that the load bus voltage would attain its rated value. To do so, the constant voltage is calculated based on (1), and if the other buses can exactly predict this voltage, not only does the load voltage return to its nominal value but also the power sharing task is performed properly. Thus, an approach is proposed here for the other resources to predict following the system steady state attained by the primary control loop. The block diagram of this approach is shown in Fig. 4. It can be seen that once the current derivative equals zero or becomes less than a small predetermined value, this condition is interpreted as the steady state and the

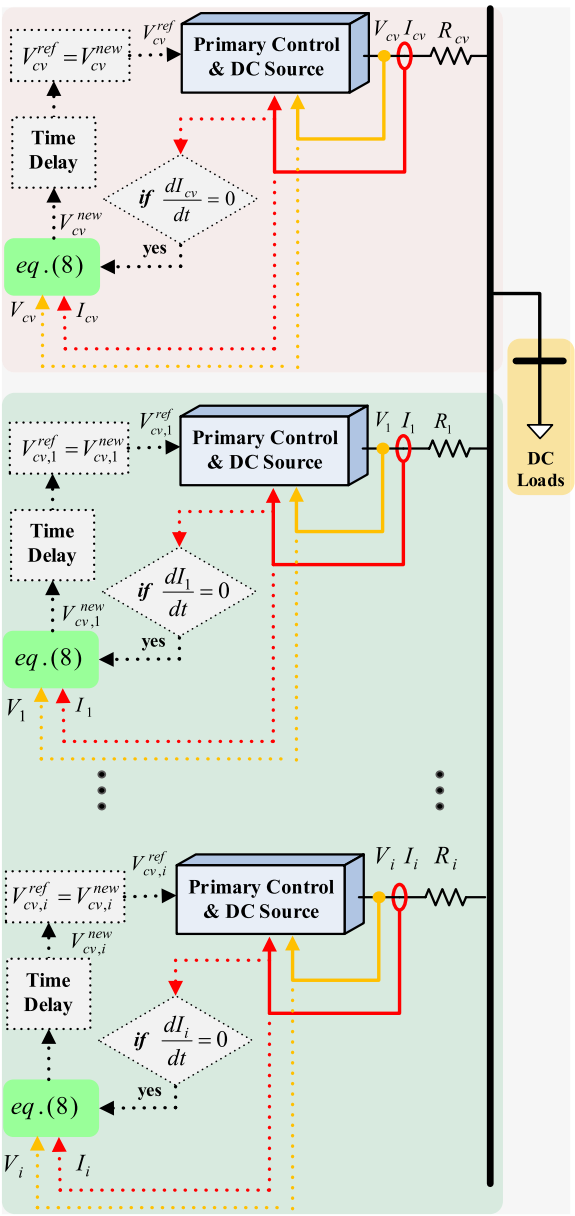

Fig. 4 Block diagram of the proposed secondary control approach without any communication link

secondary control is initiated. Otherwise, the reference voltage is not updated and the remaining converters are adjusted at the previous set-points. Note that in determination of the steady state situation, there may be some spikes because of derivative blocks that are removed by an internal algorithm in simulation studies. Once the MG reaches the steady-state conditions, (1) that defines the desired power ratio of the converters, is substituted in (5) as the target of secondary control. Accordingly, a quadratic relationship is obtained as follows:

$$V_{cv}^{new2} - V_n V_{cv}^{new} - \frac{R_{cv}}{k_i} V_i I_i = 0 \tag{7}$$

Solving (7) for V_{cv}^{new} yields the following expression:

$$V_{cv}^{new} = \frac{V_n + \sqrt{V_n^2 + 4\frac{R_{cv}}{k_i} V_i I_i}}{2} \tag{8}$$

In fact, (8) determines the reference bus voltage value to settle the bus voltage at the rated value. If (8) coincides with the droop characteristics revealed in (4), the *ith* converter output voltage is represented as:

$$V_i^{new} = V_n + R_i I_i^{new} \tag{9}$$

In this condition, the power sharing is influenced by the cable impedances and hence no satisfactory performance is achieved. In other words, the power sharing is not fulfilled based on the rated power of the converters. To avoid this issue, it can be seen that following the load change, the reference bus voltage remains constant until the steady-state condition is reached (see Fig. 4). Following the steady-state condition, the updated voltage of the reference bus is then determined based on (8) such that the load voltage is settled at the nominal value. As there is a time difference between the converters in settling into the steady-state conditions, there would also be a time difference in acquiring the updated voltage set-points between the converters. This time difference hinges on the time constant of different resources and can be estimated considering their characteristics.

Herein, a hybrid control approach based on primary and secondary controls is proposed for islanded DC-MGs which first provides an appropriate load power sharing task between the DERs like the conventional methods of this era. However, the main difference is associated with the objectives of the primary (load power sharing task between the DERs) and secondary (recovering the bus voltages to nominal values) controls which are realized simultaneously and hence the system returns to its normal state as soon as possible, while the secondary control of the conventional methods cannot fully meet this challenging task or needs extended data sharing throughout the LBC links. Moreover, in the proposed approach, to meet the secondary control task, only one signal is shared among sources throughout the LBC links. This enhances the reliability of the system, as the deployed LBC links transfer much less data in comparison with the methods in the literature. Furthermore, in this paper, another communication-less secondary control approach is devised which plays a backup role for the first in the case of failure in communication links with a short delay. Consequently, the proposed control approach not only

Table 1 System data and cable impedances

Values	Parameters
P_1	$2kW$
P_2	$4kW$
P_3	$3kW$
R_1	0.05Ω
R_2	0.1Ω
R_3	$0.075\,\Omega$
V_n	$100\,V$

can fully and quickly meet the secondary control task but also improves the reliability of the system.

4 Results and discussion

To evaluate the performance of the proposed approach, the MG shown in Fig. 1 is simulated on the MATLAB/Simulink platform. In the studies, three Proton Exchange Membrane Fuel Cells (PEMFCs) are considered as the parallel-connected DERs, and are connected to the MG through DC-DC converters. Detailed system data and cable impedances are reported in Table 1. Note that the second converter is assigned as the reference bus with V_{cv}. With respect to Table 1, $K_1 = 0.5$ and $K_3 = 0.75$. The load is of a constant power type that is changed from 3 to 6 kW at 10 s. Performance of the proposed primary control approach is tailored as the first case, and then the proposed secondary control approaches are individually explored in cases 2 and 3.

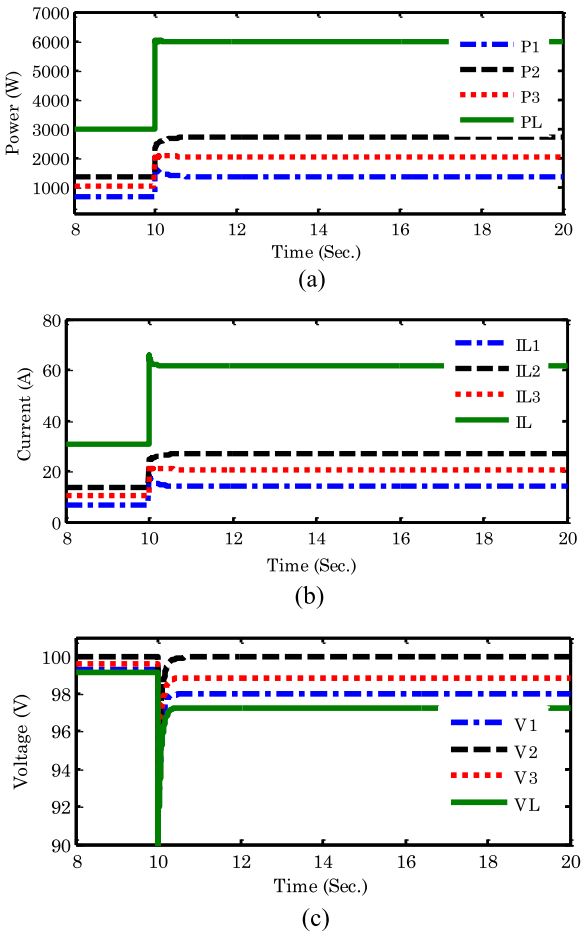

Fig. 5 Performance of the proposed primary control method, (**a**) Output power, (**b**) Output current, (**c**) Output voltages of the converters and load voltage

4.1 Case 1: Exploring the performance of the primary control approach

As mentioned, the proposed primary control approach is one which provides a proper load power sharing between the converters in DC-MG. The established control system shown in Fig. 2 is implemented in the simulation studies. Figure 5 displays the results for the power, current, and voltage signals. In this figure, the second converter denoted by *V2* and *I2* is assigned as the reference bus with constant voltage. Subscript "L" refers to the load variables. Before the load change, the output powers of the converters are $P_1 = 672.9kW$, $P_2 = 1345.8kW$, and $P_3 = 1009.4kW$. Following the load increase at 10 s, the output power of the converters is increased to meet the load requirement, and hence $P_1 = 1359kW$, $P_2 = 2717.9kW$, and $P_3 = 2038.4kW$. This confirms the performance of the proposed primary control approach. As $P_1 = k_1P_2$ and $P_3 = k_3P_2$, the power sharing task is fulfilled considering their rated power ratios.

With respect to the results in Fig. 5a, it can be seen that the power generated by the DERs is more than the required load power. The difference is due to the power losses dissipated in the cable resistances. Note that the proposed primary control approach properly shares the power losses between the DERs. This is similar to that observed on the load current sharing in Fig. 5b. However, as the objective is to share the load power, the load current sharing is not exactly performed based on rated power ratios, as Fig. 5c reveals that the load voltage is not exactly the nominal 100 V and has some deviations. Moreover, the voltage deviation increases following the increase in the load power at 10 s. To improve the load voltage, the secondary control is triggered.

4.2 Case 2: Secondary control based on LBC link

In this case, an LBC link is deployed to transfer the value of the reference bus voltage to the remaining converters, and the control system represented in Fig. 3 is considered. In the simulations, a time delay of 20 ms is considered, and the results are shown in Fig. 6. From the

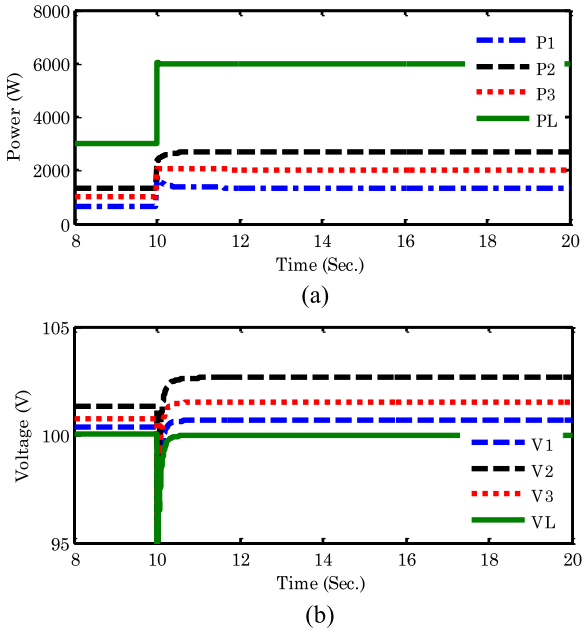

Fig. 6 Performance of the proposed secondary control based on LBC, (**a**) Output power of the converters and load power, (**b**) Output voltages of the converters and load voltage

output power of the converters in Fig. 6a, it can be seen that the established secondary control based on LBC link provides satisfactory performance on the power sharing task.

From the voltages of the DER converters and the load shown in Fig. 6b, it can be seen that the load voltage, as represented by the solid line, is exactly settled at the nominal voltage following the load change at 10 s. This confirms the anticipated performance of the proposed secondary controller.

In the applications with LBC links, it is necessary to explore the impact of possible communication delays on the performance of the investigated system. Figure 7 portrays the performance of the proposed secondary controller considering different communication delays of 20 ms, 200 ms, and 2 s. As can be seen, for the large communication delays of 2 s, there is a larger transient voltage deviation. However, the overall performance of the control system is satisfactory.

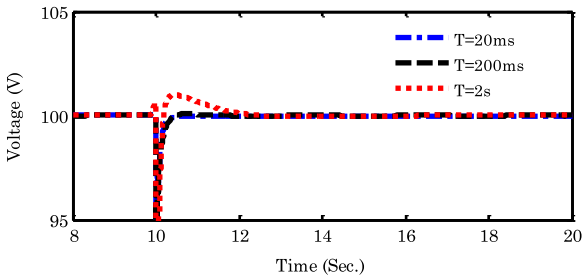

Fig. 7 Effect of communication delay on load voltage

4.3 Case 3: Secondary control approach without LBC links

In the case of the proposed secondary control approach without any communication link (see Fig. 4), once the current settles in its steady state condition, the reference voltage value is updated after 1 s time delay. It should be noted that in the simulations, the investigated DERs are of the same type with different power ratings. Accordingly, they are aligned with similar steady state conditions. However, if DERs are of different types, their steady state behaviors and time constants should be carefully determined. In this way, the considered time delay may be larger than the one designated in this study. Figure 8 demonstrates the activation time of the control circuit in each of the simulated DER converters. As can be seen, the DERs reach their steady-state conditions at different times and hence different activation times of converter control circuits are recorded. The other important observation from Fig. 8 is that the control circuits of all DERs result in similar reference voltages following the load change. This confirms the satisfactory response of the proposed control approach. The results are shown in Fig. 9. From Fig. 9a, following the load change at 10 s, the power contribution of each DER is initially determined based on the established primary control approach, and their output power changes accordingly to supply the load requirement. Thus this task is fulfilled considering the rated power of each DER. However, Fig. 9b demonstrates that the load voltage fails to follow the rated value. Then, at around 14 s with a small delay, the secondary control approach is triggered to return the load voltage to the rated value. The results confirm the performance of the proposed secondary control in providing a proper voltage control process. It is evident that the reference voltage of converter 2 is updated and the remaining converters modify their output voltages accordingly.

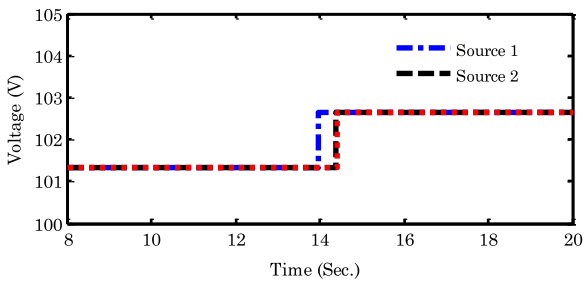

Fig. 8 Activation time of DERs and the updated reference voltage value

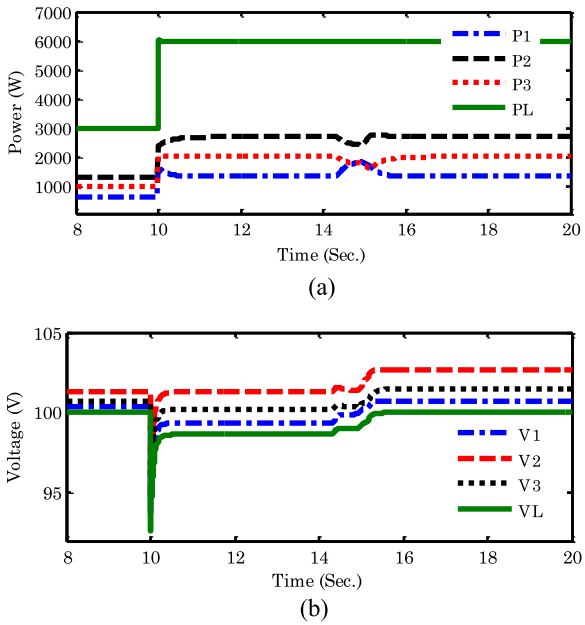

Fig. 9 Performance of the proposed primary control approach and the secondary control without communication link, (**a**) Output power of the converters and load power, (**b**) Output voltages of the converters and load voltage

4.4 Comparison

To provide a better understanding of the proposed approach, the numerical data of the three investigated cases, namely without the secondary control, with secondary control based on LBC links, and with secondary control but without LBC link, are extracted from the simulation results in Figs. 5, 6, and 9, and reported in Tables 2, 3, and 4, respectively.

In Table 2, the load voltage is not settled at the rated value of 100 V and the deviation increases as the load is increased. However, the primary control approach has established a good power sharing task based on the resource ratings. For the rated power in Table 1 and the power contribution of each resource in Table 2, it can be deduced that the load power is exactly shared between the resources based on their rated power ratios. As the voltage of the second DER is at a constant value, the load bus voltage has deviated against the nominal value.

Table 2 System data primary control approach

	Parameter			
	Voltage (V)		Power (W)	
Time	< 10 s	> 10 s	< 10 s	> 10 s
DG1	99.33	97.98	672.7	1358
DG2	100	100	1346	2715
DG3	99.61	98.83	1009	2036
Load	99.11	97.28	3000	6000

Table 3 System data primary and secondary control approach with LBW communication link

	Parameter			
	Voltage (V)		Power (W)	
Time	< 10 s	> 10 s	< 10 s	> 10 s
DG1	100.3	100.7	672.7	1358
DG2	101.3	102.6	1346	2715
DG3	100.8	101.5	1009	2036
Load	100	100	3000	6000

In Table 3, the voltages and the output power of the resources under the operation of both the primary and secondary control loops with LBC links are reported. As can be seen, the load voltage is settled at its steady-state value and the power is shared based on their ratings. However, this approach demands a communication infrastructure based on LBC.

In Table 4, in the case of secondary control without an LBC communication link, performed on the basis of voltage estimation, the system response demonstrates a 4.2 s delay in comparison to the approach based on LBC links. In this approach, immediately following the load switch at 10 s, the system reaches its steady-state conditions with only the primary control loop being active. In this process, as the voltage of the second resource is considered as constant, the voltages of other resources and that of the bus bar are fluctuating. However, the power sharing task is fulfilled satisfactorily. After reaching the steady-state condition at 14.2 s, the secondary control computes the desired voltage with respect to the new parameters and also shares the power based on the ratings of the resources. Consequently, the load voltage is retained at its rated value.

In summary, in the case where only the primary control is activated as shown in Table 2, the power sharing task is well-performed, although the load bus voltage is not settled at the nominal voltage. To retain the load bus voltage at the nominal value, the secondary control loop is triggered as shown in Tables 3 and 4 for the two proposed approaches. The first approach necessitates the presence of an LBC link, although only a voltage signal is transferred. Thus, compared to similar communication-based approaches, the proposed approach results in a lower communication burden, which justifies the application of LBC links with higher reliability. In the second proposed approach, the communication infrastructure is excluded and the control system

Table 4 System data primary and secondary control approach without communication link

	Parameter					
	Voltage (V)			Power (W)		
Time	< 10 s	> 10 s & < 14.2 s	> 14.2 s	< 10 s	> 10 s & < 14.2 s	> 14.2 s
DG1	100.3	99.33	100.7	672.8	1358	1358
DG2	101..3	101.3	102.6	1346	2716	2715
DG3	100.8	100.2	101.5	1009	2037	2036
Load	100	98.65	100	3000	6000	6000

deploys the local voltage parameters to estimate the desired voltage for the constant voltage bus. In this case, the load voltage reaches its nominal value after 4.2 s. From Table 4, it can be seen that during the delay time, the primary control ensures a successful power sharing and only the load voltage has some deviations against its nominal value. The voltage deviation is then curbed following the activation of the secondary control loop and hence the overall performance of the proposed control circuit is validated.

As pointed out earlier, this paper presents a combined and simultaneous method for the primary and secondary control tasks with the aim of keeping the bus voltage at the nominal value. To investigate the performance of this control method, the bus voltage values in both proposed methods in this paper are also compared with those in the conventional methods [24, 27, 28]. Considering the same testbed, in the conventional control method, when the load power increases by 70%, the bus voltage faces a 4.4% drop. In the presented approach in [27], which is based on LBC links, although the first aim of the paper is tackled by dividing the power according to the nominal values of the sources, still the bus voltage drops by 8%. Other studies such as the one in [24] needs the sharing of the bus voltage values among all sources in the MG. The enhanced method in [28] cannot keep the bus voltage at the nominal value. In contrast, our results show that the proposed approach can meet the task of sharing the power according to the nominal power ratings of the sources, and recover the bus voltages to the nominal value very quickly without operator intervention. In addition, as can be seen, only one signal is shared among the sources in the proposed method throughout the LBC links. In the case of failure in the communication links, the second proposed approach can play a backup role for the first with a short delay. Therefore the reliability of the system is enhanced.

5 Conclusion

This paper proposed a hybrid control approach for proper load power sharing between the converters in DC-MGs, based on their rated power ratios. In the primary control approach, the output voltage of one of the DERs is assigned as the reference voltage and this is the base of voltage control for the remaining converters. Following the load change, it is shown that load voltage deviates from its rated value and so two different secondary control loops with different topologies are proposed for suppressing the load voltage deviations. In the first approach, based on communication links, it is shown that the LBC links provide an effective approach to inform the DERs of the updated voltage reference. The effect of communication delay is assessed and it is shown that larger delay results in a longer time for the MG to settle into its steady state conditions. In this paper, another approach without dependency on communication links is also developed, in which following the steady state conditions of primary control, the proposed control algorithm estimates the reference bus voltage and updates it accordingly. It is shown that it can effectively return the load voltage to the rated value. Simulation results confirm the performance of the proposed primary control, and the effectiveness of both secondary control approaches in curbing the voltage deviations. As there are different varieties of MGs with different topologies, each of the proposed approaches could be effectively deployed in different cases.

Abbreviations

DC: Direct current; MGs: Microgrids; DERs: Distributed energy resources; AC: Alternative current; MGCC: MG central controller; LBC: Low-bandwidth communication; PEMFCs: Proton exchange membrane fuel cells.

List of symbols

i: Index of the *i*th DER converter; cv : Index of constant voltage converter.

Parameters and variables

V_i : Voltage of the *i*th DER converter; I_i : Output current of the *i*th DER converter; P_i : Active power of the *i*th DER converter; R_i : Impedance of cable connecting the *i*th converter to the load bus; K_i : Ratio of the active power rating of the *i*th DER converter to converter with constant voltage; V_{cv}

: Voltage of converter with constant voltage regarding to the load bus; I_{cv} : Output current of converter with constant voltage regarding to the load bus; P_{cv} : Active power of converter with constant voltage regarding to the load bus; R_{cv} : Impedance of cable connecting the converter with constant voltage to the load bus; V_n : Nominal load bus voltage; G_d : Transfer function for communication time delay; τ : Time delay.

Acknowledgements
There is not any acknowledgements to report.

Author contributions
VM have contributions on modeling, simulations, performing the analysis and writing the paper. SG have contributions on modeling, simulations, performing the analysis and writing the paper. EP have contributions on modeling, simulations, performing the analysis and writing the paper. AY have contributions on modeling, simulations, performing the analysis and writing the paper. All authors read and approved the final manuscript.

Funding
No funding.

Availability of data and materials
As per requested from corresponding author.

Declarations

Competing interest
The authors declare that they have no known competing financial interests or personal relationships that could have appeared to influence the work reported in this paper.

Author details
[1]School of Electrical and Computer Engineering, University of Tehran, 16th Azar St., Enghelab Sq., Tehran, Iran. [2]Electrical Engineering Department, Urmia University, 11Km SERO Road, Urmia City, Iran. [3]Department of Electrical Engineering and Automation, Aalto University, Aalto University Foundation sr, PO BOX 11000, FI-00076 Aalto, Finland. [4]Department of Electrical Engineering, Shahid Rajaee Teacher Training University, Shabanlou, QFJR+2MP, Tehran, Tehran Province, Iran.

Received: 7 July 2022 Accepted: 15 October 2022
Published online: 27 October 2022

References

1. Anjaiah, K., Dash, P. K., & Sahani, M. (2022). A new protection scheme for PV-wind based DC-ring microgrid by using modified multifractal detrended fluctuation analysis. *Protection and Control of Modern Power Systems, 7*(1), 1–24.
2. Teimourzadeh, S., Aminifar, F., & Shahidehpour, M. (2017). Contingency-constrained optimal placement of micro-PMUs and smart meters in microgrids. *IEEE Transactions on Smart Grid, 10*, 1889–1897.
3. Abedini, M., Moradi, M. H., & Hosseinia, S. M. (2016). Optimal clustering of MGs based on droop controller for improving reliability using a hybrid of harmony search and genetic algorithms. *ISA Transactions, 61*, 119–128.
4. Justo, J. J., Mwasilu, F., Lee, J., et al. (2013). AC-microgrids versus DC-microgrids with distributed energy resources, A review. *Renewable and Sustainable Energy Reviews, 24*, 387–405.
5. Elsayed, A. T., Mohamed, A. A., & Mohammed, O. A. (2015). DC microgrids and distribution systems. *Electric Power Systems Research, 119*, 407–417.
6. Jian, Z. H., He, Z. Y., Jia, J. et al. (2013). A review of control strategies for DC micro-grid. *Paper presented in Fourth International Conference on Intelligent Control and Information Processing*, Beijing, China 9–11 June 2013.
7. Boeke, U., Wendt, M. (2015). DC power grids for buildings. *IEEE First International Conference in DC Microgrids*, Atlanta, GA, USA, 7-10 June 2015, 210-214.
8. Fregosi, D., Ravula, S., Brhliket, D. et al. (2015). A comparative study of DC and AC microgrids in commercial buildings across different climates and operating profiles. *IEEE First International Conference in DC Microgrids*, Atlanta, GA, USA, 7–10 June 2015, 159–164.
9. Mortezapour, V., & Lesani, H. (2017). Hybrid AC/DC microgrids: A generalized approach for autonomous droop-based primary control in islanded operations. *International Journal of Electrical Power & Energy Systems, 93*, 109–118.
10. Badal, F. R., Das, P., Sarker, S. K., & Das, S. K. (2019). A survey on control issues in renewable energy integration and microgrid. *Protection and Control of Modern Power Systems, 4*(1), 1–27.
11. Yang, N., Paire, D., Gao, F., et al. (2015). Compensation of droop control using common load condition in DC microgrids to improve voltage regulation and load sharing. *International Journal of Electrical Power & Energy Systems, 64*, 752–760.
12. Farhadi, M., & Mohammed, O. A. (2015). Performance enhancement of actively controlled hybrid DC microgrid incorporating pulsed load. *IEEE Trans on Industry Applications, 51*(5), 3570–3578.
13. Boroojeni, K., Amini, M. H., Nejadpak, A., et al. (2016). A novel cloud-based platform for implementation of oblivious power routing for clusters of microgrids. *IEEE Access on The Internet of Energy: Architectures, Cyber Security, and Applications, 5*, 607–619.
14. Amini, M. H., Boroojeni. K., Dragičević. T. et al. (2017). A comprehensive cloud-based real-time simulation framework for oblivious power routing in clusters of DC microgrids. *IEEE Second International Conference on DC Microgrids*, Nuremburg, Germany, 27–29 June 2017.
15. Azimi, S. M., & Afsharnia, S. (2016). Multi-purpose droop controllers incorporating a passivity-based stabilizer for unified control of electronically interfaced distributed generators including primary source dynamics. *ISA Transactions, 63*, 140–153.
16. Teimourzadeh, S., Davarpanah, M., Aminifar, F., et al. (2018). An adaptive auto-reclosing scheme to preserve transient stability of microgrids. *IEEE Transactions on Smart Grid, 9*(4), 2638–2646.
17. Nasirian, V., Moayedi, S., Davoudi, A., et al. (2015). Distributed cooperative control of DC microgrids. *IEEE Transactions on Power Electronics, 30*(4), 2288–2303.
18. Wang, P., Lu, X., Yang, X., et al. (2016). An improved distributed secondary control method for DC microgrids with enhanced dynamic current sharing performance. *IEEE Trans Power Electronics, 31*(9), 6658–6673.
19. Guerrero, J. M., Vasquez, J. C., Matas, J., et al. (2011). Hierarchical control of droop-controlled AC and DC microgrids - A general approach toward standardization. *IEEE Transactions on Industrial Electronics, 58*(1), 158–172.
20. Shafiee, Q., Guerrero, J. M., & Vasquez, J. C. (2014). Distributed secondary control for islanded microgrids-a novel approach. *IEEE Transactions on Power Electronics, 29*(2), 1018–1031.
21. Anand, S., Fernandes, B. G., & Guerrero, J. M. (2013). Distributed control to ensure proportional load sharing and improve voltage regulation in low-voltage DC microgrids. *IEEE Transactions on Power Electronics, 28*(4), 1900–1913.
22. Lu, X., Guerrero, J. M., Sun, K., et al. (2014). An improved droop control method for DC microgrids based on low bandwidth communication with DC bus voltage restoration and enhanced current sharing accuracy. *IEEE Transactions on Power Electronics, 29*(4), 1800–1812.
23. Nasirian, V., Davoudi, A., Lewis, F. L., et al. (2014). Distributed adaptive droop control for DC distribution systems. *IEEE Transactions on Energy Conversion, 29*(4), 944–956.
24. Golshannavaz, S., & Mortezapour, V. (2018). A generalized droop control approach for islanded DC microgrids hosting parallel-connected DERs. *Sustainable Cities and Society, 36*, 237–245.
25. Ghalebani, P., & Niasati, M. (2018). A distributed control strategy based on droop control and low-bandwidth communication in DC microgrids with increased accuracy of load sharing. *Sustainable Cities and Society', 40*, 155–164.
26. Loh, P. C., Blaabjerg, F., Peyghami-Akhuleh, S. et al. (2016). Distributed secondary control in DC microgrids with low-bandwidth communication link', *Power Electronics and Drive Systems Technologies Conference (PEDSTC)*.

27. Khorsandi, A., Ashourloo, M., & Mokhtari, H. (2014). A decentralized control method for a low-voltage DC microgrid. *IEEE Transactions on Energy Conversion, 29*(4), 793–801.
28. Mi, Y., Guo, J., et al. (2021). A power sharing strategy for islanded DC microgrid with unmatched line impedance and local load. *Electric Power Systems Research, 192*, 106983.